Supporting Information

(WO+ICG)@PLGA@lipid/Plasmid DNA nanocomplex as core-shell vectors for synergistically genetic/photothermal therapy

Bai Yang[1,2,#], Guoqing Feng[2,#], Qingbin Yang[2,#], Tingting Hua[2], Bowen Li[2], Hao-Lin Guo[3], Yuan Liu[4,] , Qing Yuan[5], Niansong Qian[6,] * and Bin Zheng[2,] *

[1] Academy of Medical Engineering and Translational Medicine, Tianjin University, Tianjin, 300072, China.

[2] Department of Stomatology, Tianjin Medical University General Hospital, Heping District, Tianjin 300052, China.

[3] School of Traditional Chinese Medicine, Beijing University of Chinese Medicine, Beijing, 102401, China.

[4] Tianjin Anding Hospital, Tianjin, 300222, China.

[5] Department of Urology, The Third Medical Center, Chinese People's Liberation Army (PLA) General Hospital, Beijing 100853, China

[6] Department of Respiratory, the Eighth Medical Center of Chinese PLA General Hospital, Beijing 100853, China.

[#] These authors contributed equally to this work.

∗ Corresponding authors.

E-mail addresses: qianniansong1@163.com (N. Qian) and binzheng@tju.edu.cn (B. Zheng)

1. Experimental Section

1.1 Characterization of nanoparticles

The morphology and size of NPs were characterized by SEM (APREO, FEI) and TEM (JEM-2100F). The hydrodynamic particle size of the NPs was measured with a DLS analyzer (Malvern Zetasizer Nano ZS90).

1.2 B16-F10 cancer cell culture

In this study, B16-F10 melanoma cells were cultured under aseptic conditions. Initially, cells were revived from cryopreservation by rapid thawing at 37°C and subsequently transferred into a 15 mL centrifuge tube containing 10 mL of pre-warmed DMEM supplemented with 10% fetal bovine serum (FBS) and 1% penicillin-streptomycin, to dilute and remove cryoprotectant. The cell suspension was centrifuged at 1000 rpm for 5 min, and the supernatant was discarded. The cell pellet was resuspended in fresh DMEM with supplements and seeded in sterile culture dishes at an appropriate density for the planned experiments. The cells were then incubated in a humidified atmosphere at 37°C with 5% CO_2, and the medium was changed every two days. Upon reaching 70-80% confluence, cells were washed with phosphate-buffered saline (PBS), detached using 0.25% trypsin- ethylenediaminetetraacetic acid (EDTA) solution, and centrifuged at 1000 rpm for 5 min. After discarding the supernatant, cells were resuspended in a fresh medium and reseeded for further experiments. Throughout the culturing process, cells were

regularly monitored for morphology and signs of contamination.

1.3 In vitro cytotoxicity evaluation

Cytotoxicity of (WO+ICG)@PLGA@PL was evaluated in B16-F10 cells by standard 3-(4,5-Dimethylthiazol-2-yl)-2,5-diphenyltetrazolium bromide (MTT) assay. B16-F10 cells were treated with different concentrations of (WO+ICG)@PLGA@PL (0.0016, 0.008, 0.04, 0.2, and 1 mg/mL) for 24 h. MTT assay was used to test the cytotoxicity according to the standard protocol.

1.4 Measurement of the effect of nanoparticles on cells

To facilitate the observation of the effect of the nanoparticle packaging process on ICG expression by fluorescence imaging, as well as for the evaluation of the gene transfection effect (with GFP-labelled plasmid DNA), B16-F10 cells (1×10^5 cells) was inoculated into confocal petri dishes and incubated with different nanoparticles for 6 h. The cell uptake behavior of B16-F10 cells was observed on a Raman microscope (Thermo Scientific, DXR3xi Raman Imaging Microscope). Afterward, the nuclei of B16-F10 cells were stained with Hoechst 33342 dye. After the removal of excess dye and NPs by washing, B16-F10 cells were observed on a confocal laser scanning microscope (Leica).

2. Supplementary Figures

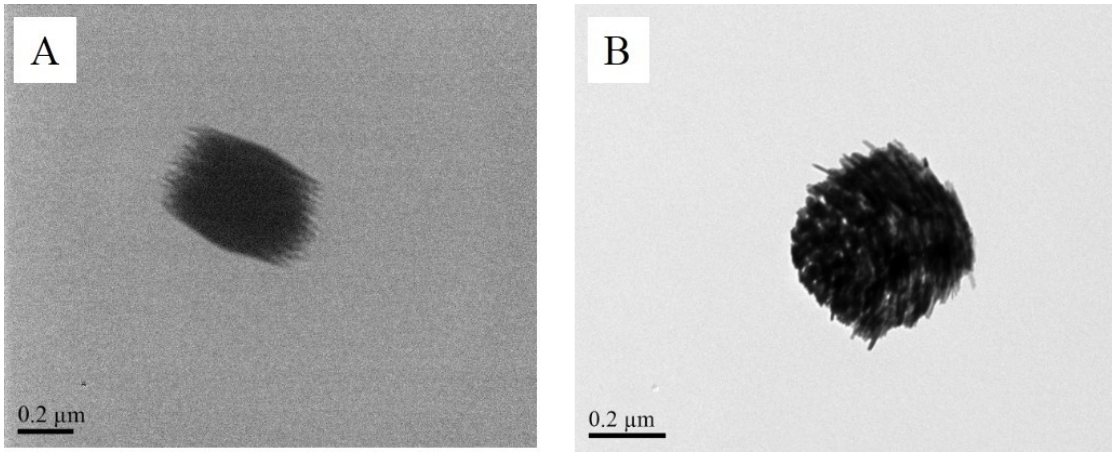

Figure S1:

(A) the TEM images of WO rod crystals.

(B) the TEM images of WO crystal dots aggregation after sonication.

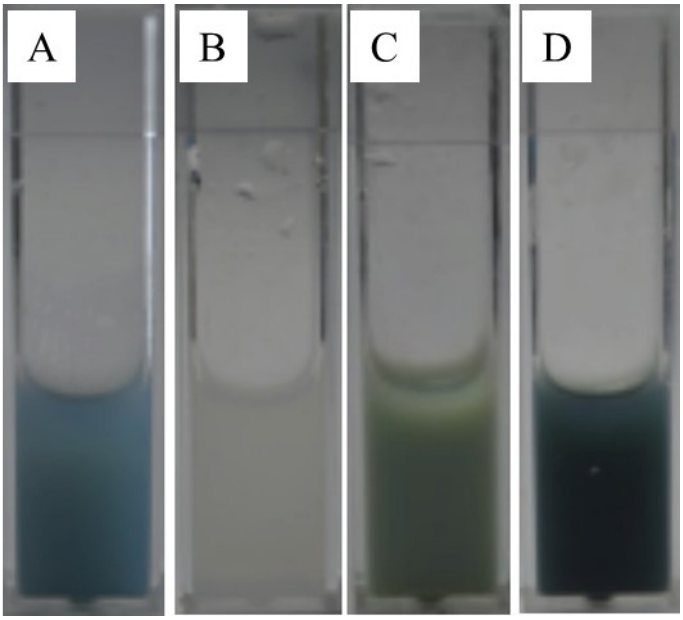

Figure S2: (A-D) the images of WO, WO@PLGA, (WO+ICG)@PLGA and (WO+ICG)@PLGA@PL in water.

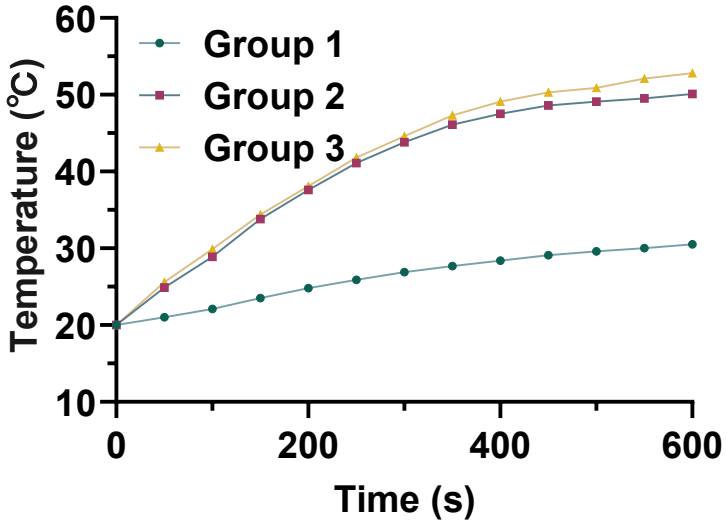

Figure S3:

The photothermal heat generation curve of Figure 4B.

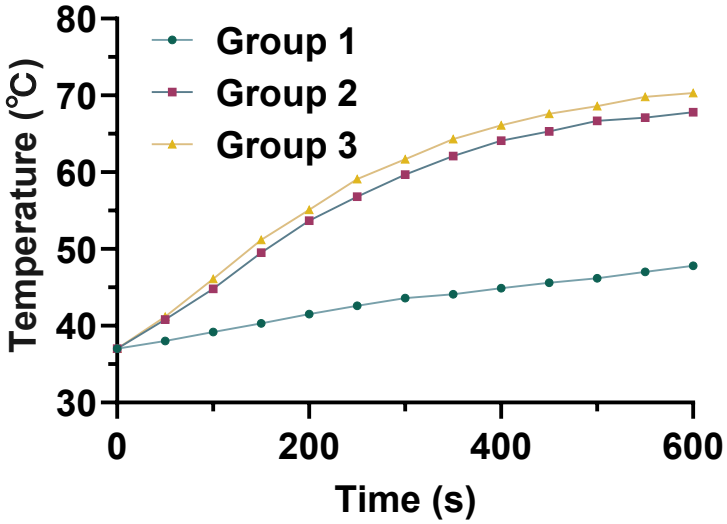

Figure S4:

The photothermal heat generation curve of Figure 4D.